Timelike vs spacelike DVCS from JLab, COMPASS to colliders and to ultraperipheral collisions at AFTER@LHC

Lech Szymanowski

Theoretical Physics Department
National Center for Nuclear Research (NCBJ), Warsaw

GDR 2012, December 6-7th

in collaboration with
H. Moutarde(CEA, Saclay), B. Pire (CPhT Ecole Polytechnique, Palaiseau),
F. Sabatie (CEA, Saclay), J. Wagner (NCBJ, Warsaw)

UPC@AFTER@LHC: J. Ph. Lansberg (IPN, Orsay), J. Wagner (NCBJ, Warsaw)

Outline

DVCS

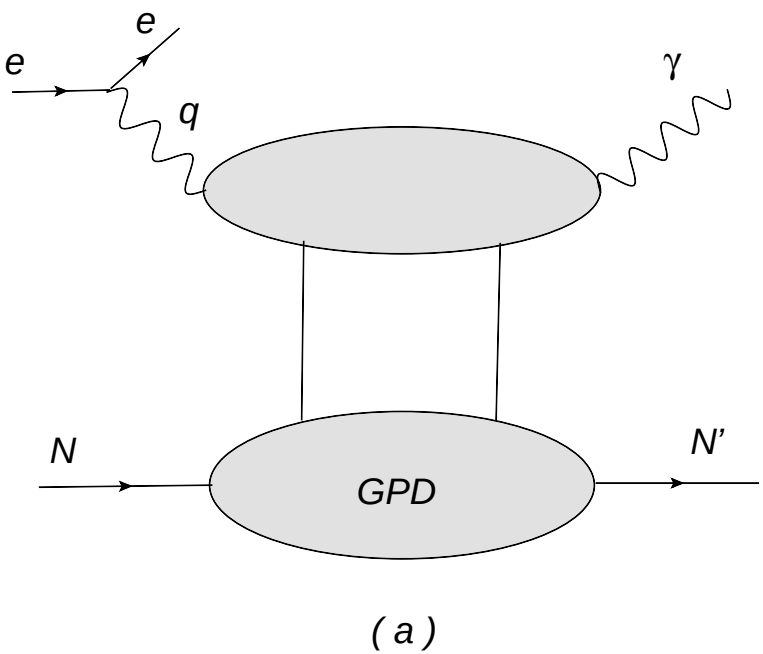

Figure: Deeply Virtual Compton Scattering : $lN \to l'N'\gamma$

TCS

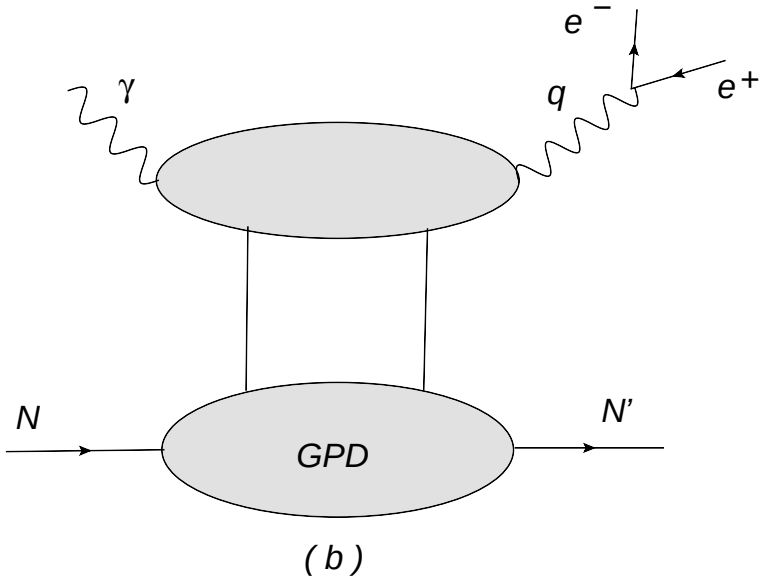

Figure: Timelike Compton Scattering: $\gamma N \to l^+ l^- N'$

Why TCS?

- GDPs enter factorization theorems for hard exlusive reactions (DVCS, deeply virtual meson production, TCS etc.), in a similar manner as PDFs enter factorization theorem for DIS
- First moment of GPDs enters the Ji's sum rule for the angular momentum carried by partons in the nucleon,
- Deeply Virtual Compton Scattering (DVCS) is a golden channel for GPDs extraction,
- Why TCS: universality of the GPDs, spacelike-timelike crossing and understanding the structure of the NLO corrections,
- Experiments *at low energy*: CLAS 6 GeV $\rightarrow$ CLAS 12 GeV, *at high energy*: COMPASS, RHIC, LHC and AFTER@LHC ?

Coordinates

Berger, Diehl, Pire, 2002

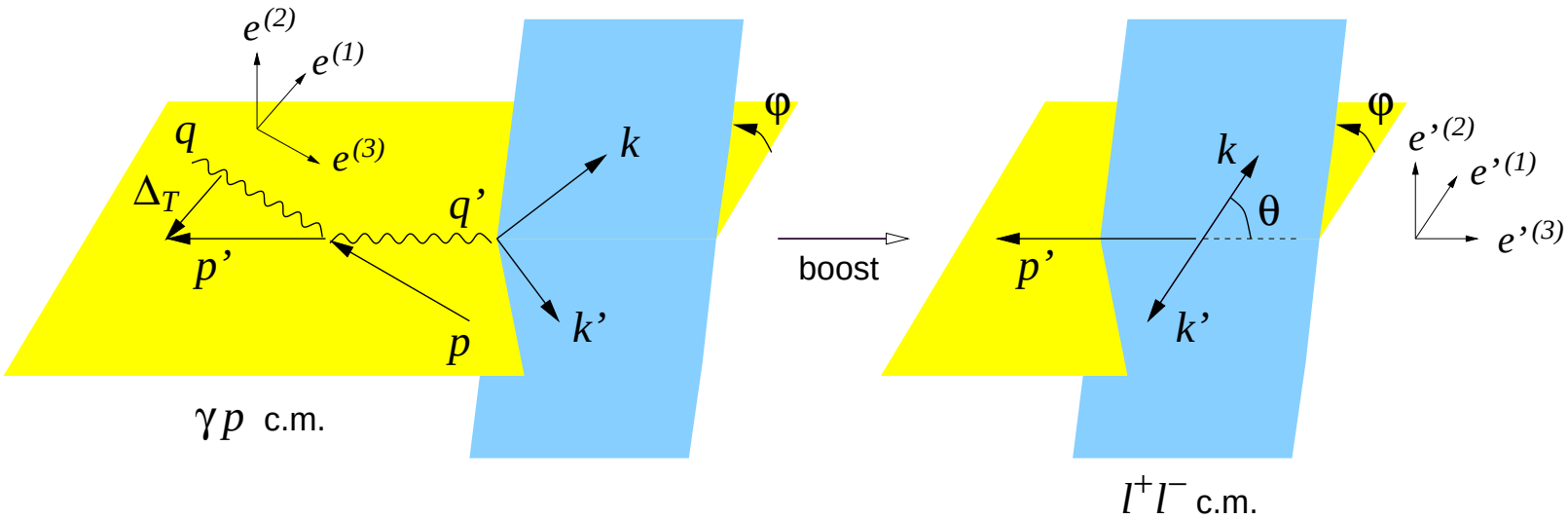

Figure: Kinematical variables and coordinate axes in the γp and $\ell^+\ell^-$ c.m. frames.

The Bethe-Heitler contribution

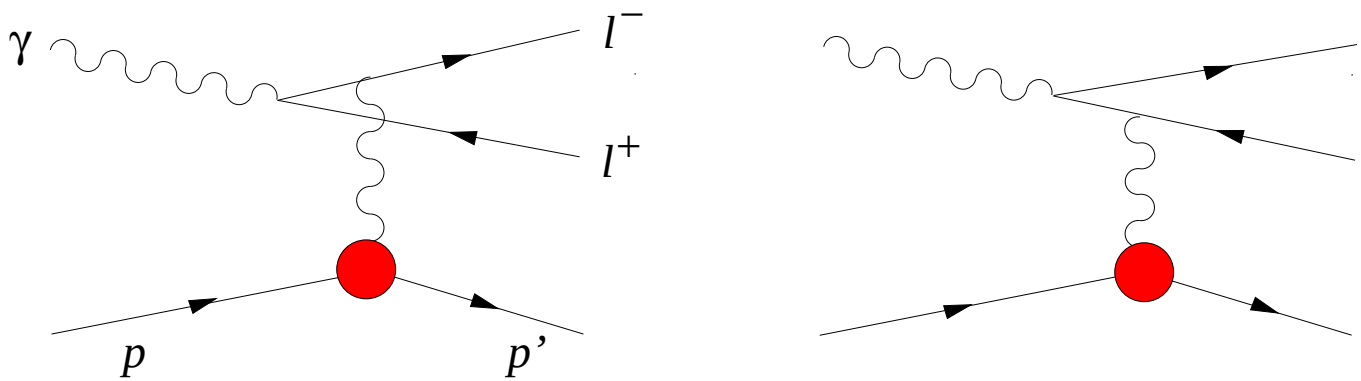

Figure: The Feynman diagrams for the Bethe-Heitler amplitude.

$$\frac{d\sigma_{BH}}{dQ'^2 dt d\cos\theta} \approx 2\alpha^3 \frac{1}{-tQ'^4} \frac{1+\cos^2\theta}{1-\cos^2\theta} \left(F_1(t)^2 - \frac{t}{4M_p^2} F_2(t)^2 \right),$$

For small θ BH contribution becomes very large

The Compton contribution

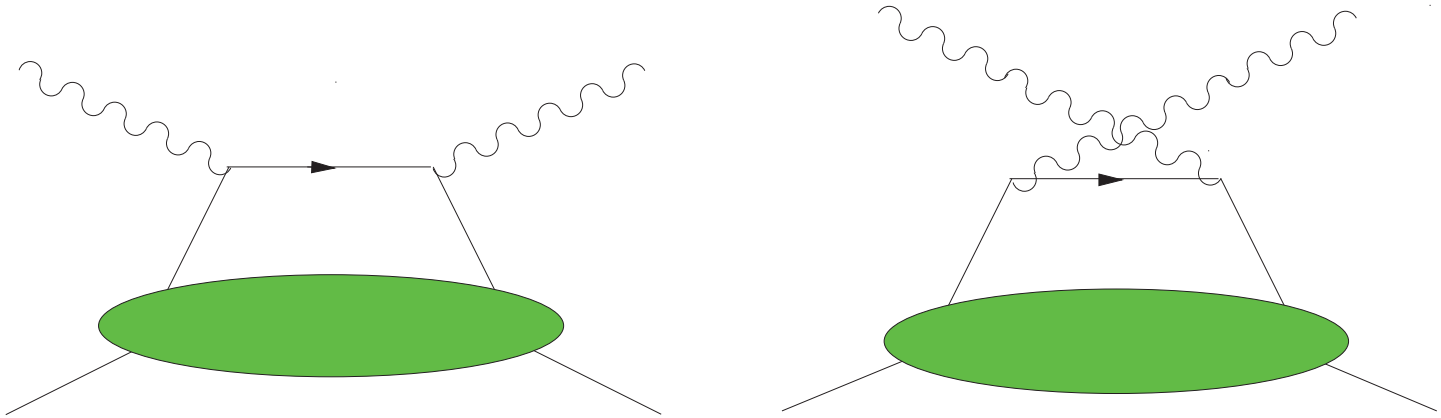

Figure: Handbag diagrams for the Compton process in the scaling limit.

$$\frac{d\sigma_{TCS}}{dQ'^2 d\Omega dt} \approx \frac{\alpha^3}{8\pi}\frac{1}{s^2}\frac{1}{Q'^2}\left(\frac{1+\cos^2\theta}{4}\right)2(1-\xi^2)\left|\mathcal{H}(\xi,t)\right|^2,$$

$$\mathcal{H}(\xi,t) = \sum_q e_q^2 \int_{-1}^{1} dx T(x,\xi,Q') H^q(x,\xi,t),$$

Interference

The interference part of the cross-section for $\gamma p \to \ell^+ \ell^- p$ with unpolarized protons and photons is given at leading order by

$$\frac{d\sigma_{INT}}{dQ'^2\, dt\, d\cos\theta\, d\varphi} \sim \cos\varphi\ \mathrm{Re}\,\mathcal{H}(\xi, t)$$

Linear in GPD's, odd under exchange of the l^+ and l^- momenta $\Rightarrow$ angular distribution of lepton pairs is a good tool to study interference term.

Berger, Diehl, Pire, 2002

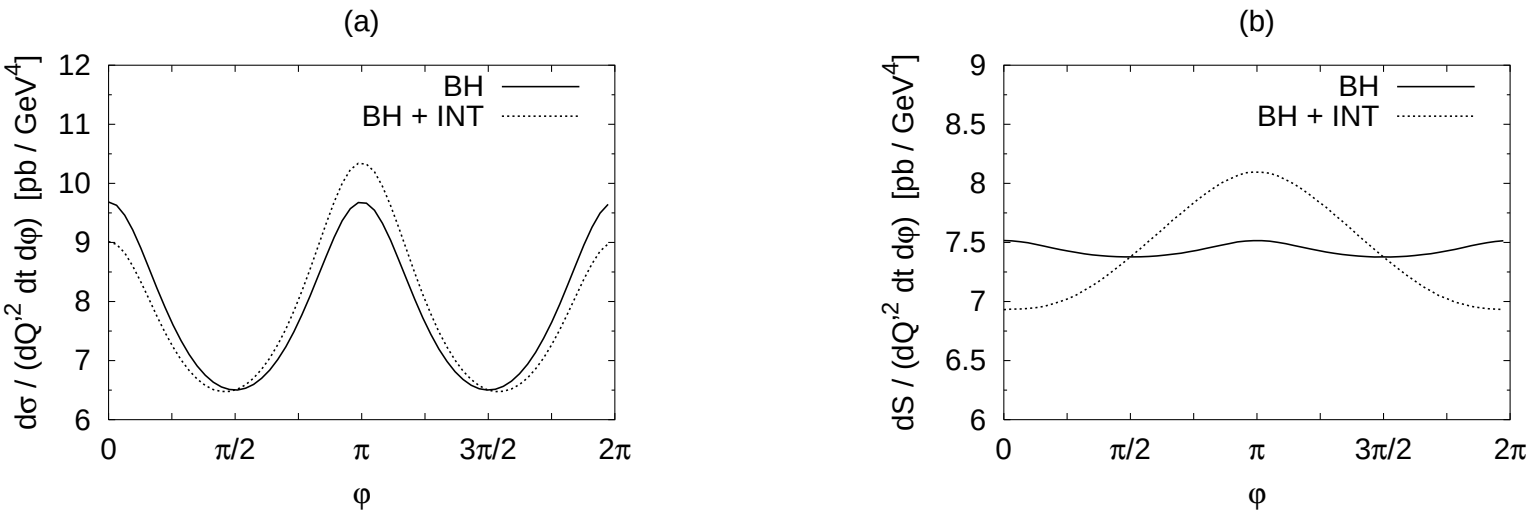

B-H dominant for small energies;

JLAB 6 GeV data

Rafayel Paremuzyan PhD thesis

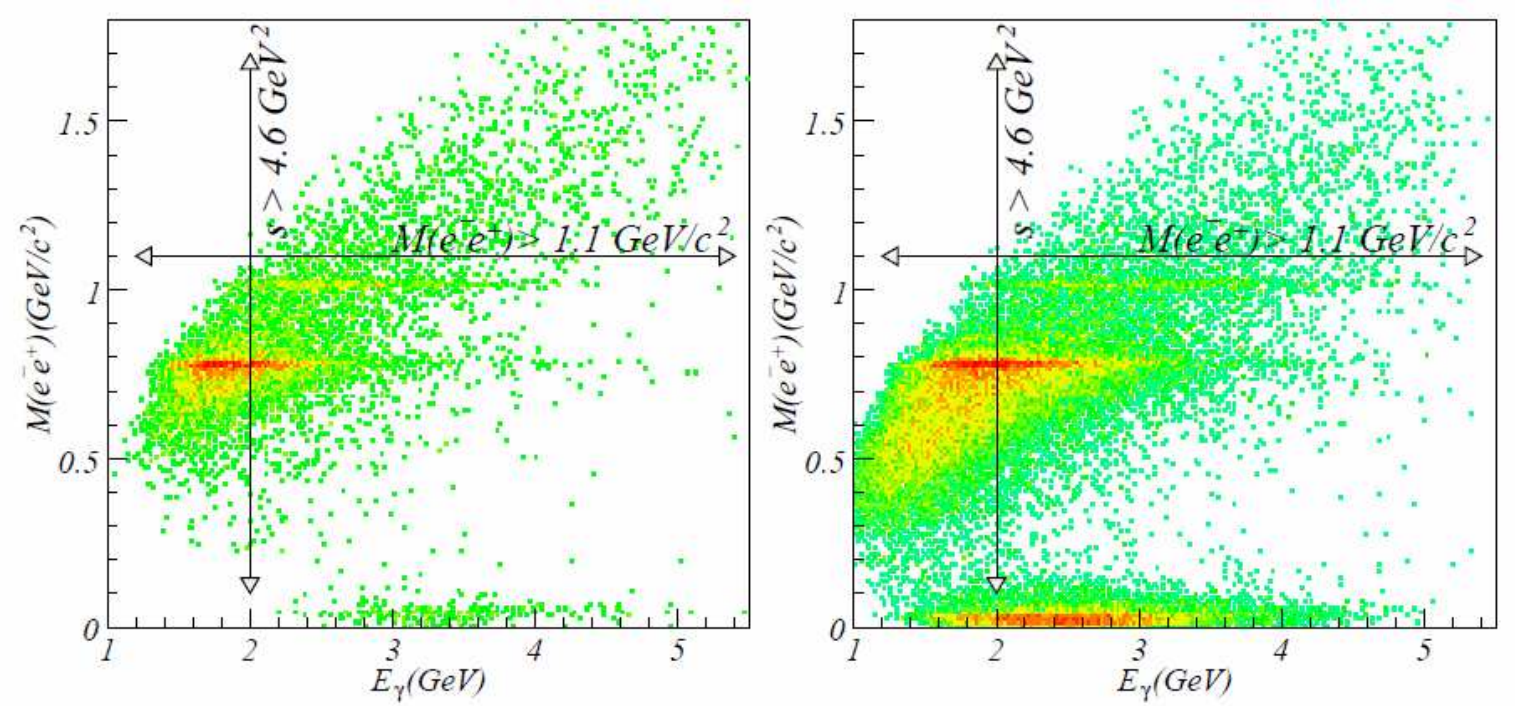

Figure: e^+e^- invariant mass distribution vs quasi-real photon energy. For TCS analysis $M(e^+e^-) > 1.1\,\mathrm{GeV}$ and $s_{\gamma p} > 4.6\,\mathrm{GeV}^2$ regions are chosen. Left graph represents e1-6 data set, right one is from e1f data set.

There is more data from g12 data set, soon to be analyzed. 12 GeV upgrade enables exploration of invariant masses up to $Q^2 = 9\,\mathrm{GeV}^2$ mass.

Theory vs experiment

R.Paremuzyan and V.Guzey:

$$R = \frac{\int d\phi \ \cos\phi \ d\sigma}{\int \ d\phi \ d\sigma}$$

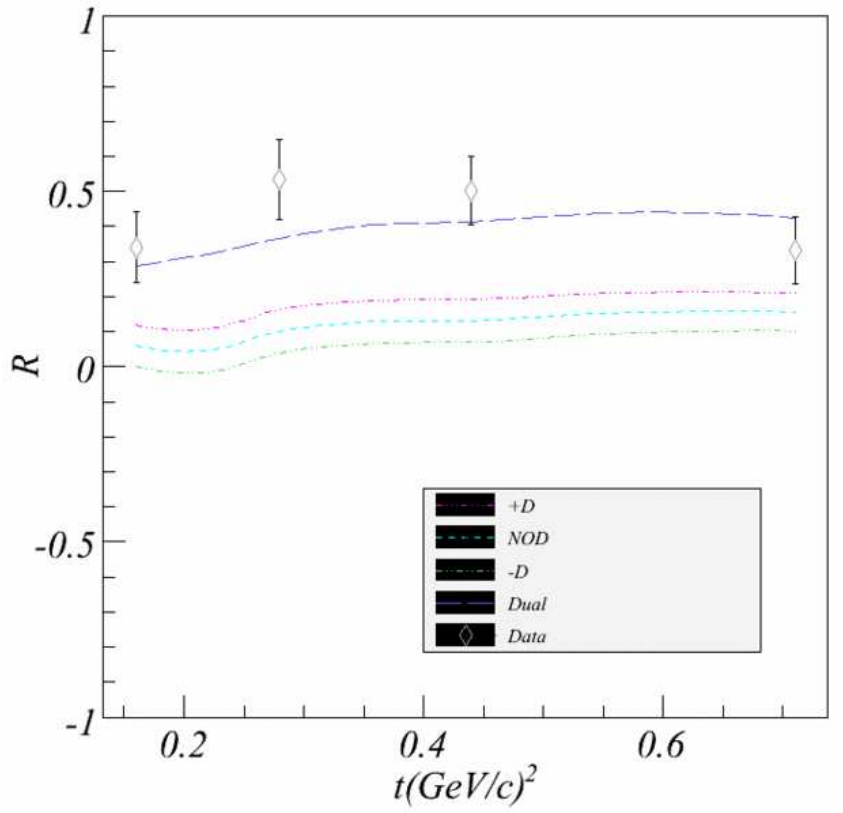

Figure: Theoretical prediction of the ratio R for various GPDs models. Data points after combining both e1-6 and e1f data sets.

Motivation for NLO

Why do we need NLO corrections to TCS:

- gluons enter at NLO,
- DIS versus Drell-Yan: big K-factors $\log \frac{-Q^2}{\mu_F^2} \to \log \frac{Q^2}{\mu_F^2} \pm i\pi,$
- reliability of the results, factorization scale dependence,

Belitsky, Mueller, Niedermeier, Schafer, Phys.Lett.B474 ,2000.
Pire, Szymanowski, Wagner, Phys.Rev.D83, 2011.

General Compton Scattering:

$$\gamma^*(q_{in})N \to \gamma^*(q_{out})N'$$

- DVCS: $q_{in}^2 < 0\,, \quad q_{out}^2 = 0$
- TCS: $q_{in}^2 = 0\,, \quad q_{out}^2 > 0$
- DDVCS: $q_{in}^2 < 0\,, \quad q_{out}^2 > 0$

Amplitude:

$$\mathcal{A}^{\mu\nu} = g_T^{\mu\nu} \int_{-1}^{1} dx \left[\sum_q^{n_F} T^q(x) F^q(x) + T^g(x) F^g(x) \right]$$

where renormalized coefficient functions are given by:

$$\begin{aligned} T^q &= C_0^q + C_1^q + \ln\left(\frac{Q^2}{\mu_F^2}\right) \cdot C_{coll}^q \,, \\ T^g &= C_1^g + \ln\left(\frac{Q^2}{\mu_F^2}\right) \cdot C_{coll}^g \end{aligned}$$

Diagrams

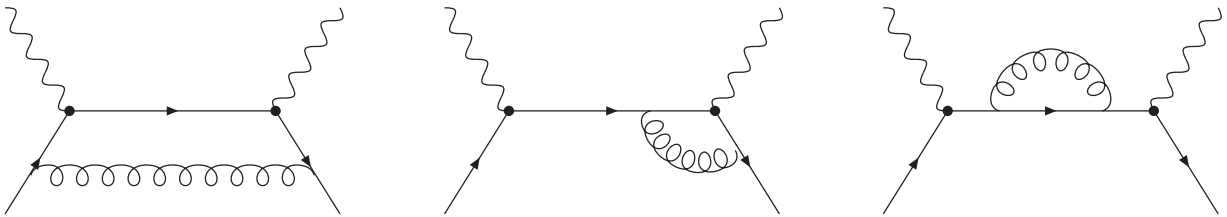

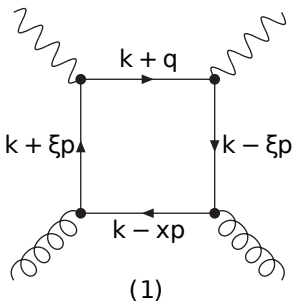

(1)

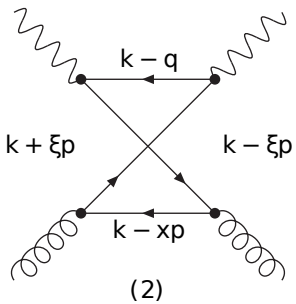

(2)

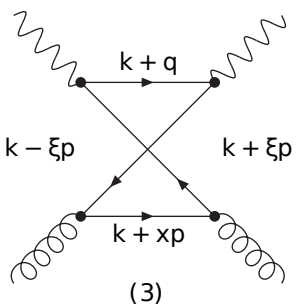

(3)

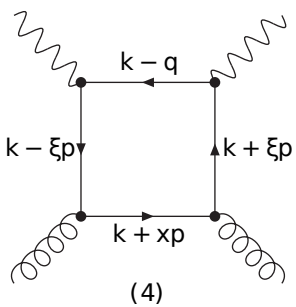

(4)

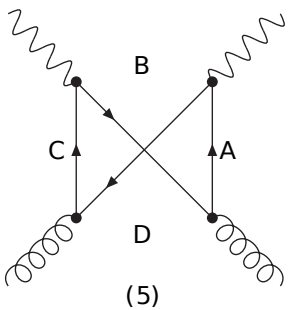

(5)

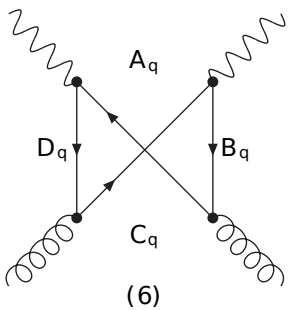

(6)

Results: TCS + DVCS + DDVCS

TCS:
Quark coefficient functions:

$$C_0^q = e_q^2 \left(\frac{1}{x-\xi-i\varepsilon} + \frac{1}{x+\xi+i\varepsilon} \right),$$

$$C_1^q = \frac{e_q^2 \alpha_S C_F}{4\pi}$$

$$\left\{ \frac{1}{x-\xi-i\varepsilon} \left[-9 + 3\log(-1+\frac{x}{\xi}-i\varepsilon) - 6\frac{\xi}{x+\xi}\log(-1+\frac{x}{\xi}-i\varepsilon) + 6\frac{\xi}{x+\xi}\log(-2-i\varepsilon) \right.\right.$$
$$\left. + \log^2(-1+\frac{x}{\xi}-i\varepsilon) - \log^2(-2-i\varepsilon) \right]$$
$$+ \frac{1}{x+\xi+i\varepsilon} \left[-9 + 3\log(-1-\frac{x}{\xi}-i\varepsilon) + 6\frac{\xi}{x-\xi}\log(-1-\frac{x}{\xi}-i\varepsilon) - 6\frac{\xi}{x-\xi}\log(-2-i\varepsilon) \right.$$
$$\left.\left. + \log^2(-1-\frac{x}{\xi}-i\varepsilon) - \log^2(-2-i\varepsilon) \right] \right\},$$

$$C_{coll}^q = \frac{e_q^2 \alpha_S C_F}{4\pi} \left\{ \frac{1}{x-\xi-i\varepsilon} \left[3 + 2\log(-1+\frac{x}{\xi}-i\varepsilon) - 2\log(-2-i\varepsilon) \right] \right.$$
$$\left. + \frac{1}{x+\xi+i\varepsilon} \left[3 + 2\log(-1-\frac{x}{\xi}-i\varepsilon) - 2\log(-2-i\varepsilon) \right] \right\}$$

Gluon coefficient functions:

$$C^g_{coll} = \frac{\left(\sum_q e_q^2\right)\alpha_S T_F}{4\pi}\frac{2}{(x+\xi+i\varepsilon)(x-\xi-i\varepsilon)}\cdot$$

$$\left[\frac{x-\xi}{x+\xi}\log\left(-1+\frac{x}{\xi}-i\varepsilon\right)+\frac{x+\xi}{x-\xi}\log\left(-1-\frac{x}{\xi}-i\varepsilon\right)-2\frac{x^2+\xi^2}{x^2-\xi^2}\log(-2-i\varepsilon)\right],$$

$$C^g_1 = \frac{\left(\sum_q e_q^2\right)\alpha_S T_F}{4\pi}\frac{1}{(x+\xi+i\varepsilon)(x-\xi-i\varepsilon)}\cdot$$

$$\begin{aligned}\Big[&-2\frac{x-3\xi}{x+\xi}\log\left(-1+\frac{x}{\xi}-i\varepsilon\right)+\frac{x-\xi}{x+\xi}\log^2\left(-1+\frac{x}{\xi}-i\varepsilon\right)\\&-2\frac{x+3\xi}{x-\xi}\log\left(-1-\frac{x}{\xi}-i\varepsilon\right)+\frac{x+\xi}{x-\xi}\log^2\left(-1-\frac{x}{\xi}-i\varepsilon\right)\\&+4\frac{x^2+3\xi^2}{x^2-\xi^2}\log(-2-i\varepsilon)-2\frac{x^2+\xi^2}{x^2-\xi^2}\log^2(-2-i\varepsilon)\Big]\end{aligned}$$

Discussion

D. Mueller, B. Pire, L. Sz. and J. Wagner, Phys. Rev. D 86

The relation between the coefficient functions for NLO DVCS and NLO TCS:

$$
\begin{aligned}
{}^{TCS}T^{q} &= {}^{DVCS}T^{q\,*} - i\pi\, {}^{DVCS}C^{q\,*}_{coll} \\
{}^{TCS}T^{g} &= {}^{DVCS}T^{g\,*} - i\pi\, {}^{DVCS}C^{g\,*}_{coll}\,.
\end{aligned}
$$

TCS: Re vs. Im parts of TCS FF

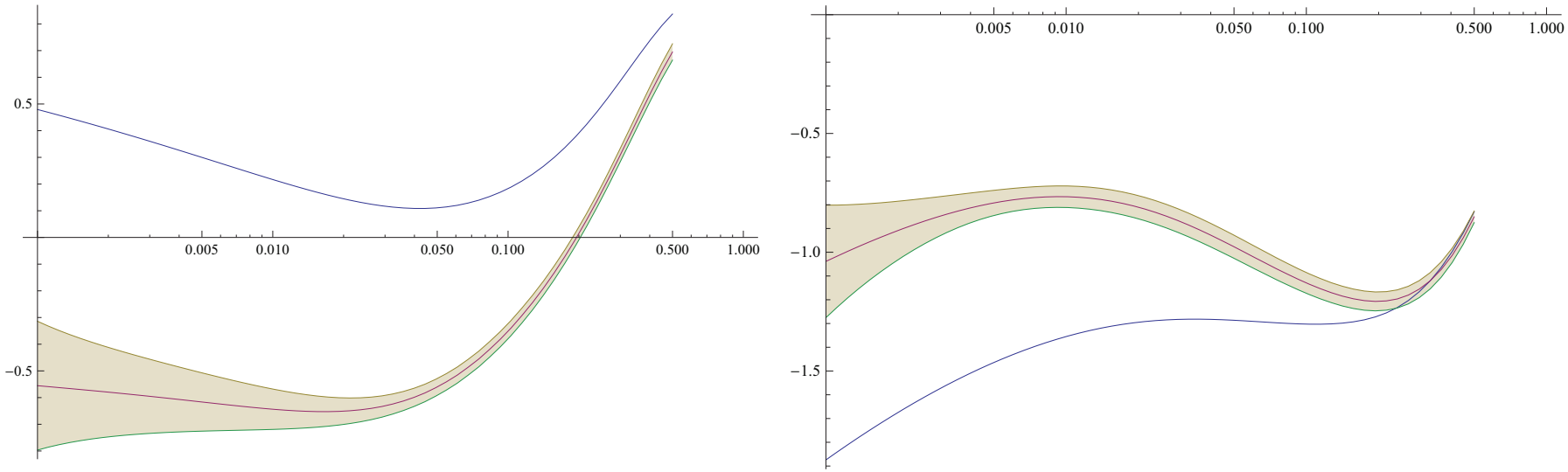

Figure: The real (left) and imaginary(right) parts of the TCS Compton Form Factor $\mathcal{H}$ multiplied by ξ, as a function of ξ in the double distribution model based on MSTW08 parametrization, for $\mu_F^2 = Q^2 = 4$ GeV^2 and $t = -0.1$ GeV^2. The shaded bands show the effect of a one sigma uncertainty of the input MSTW08 fit to the parton distributions.

TCS: LO vs. NLO-quark vs. NLO-gluon

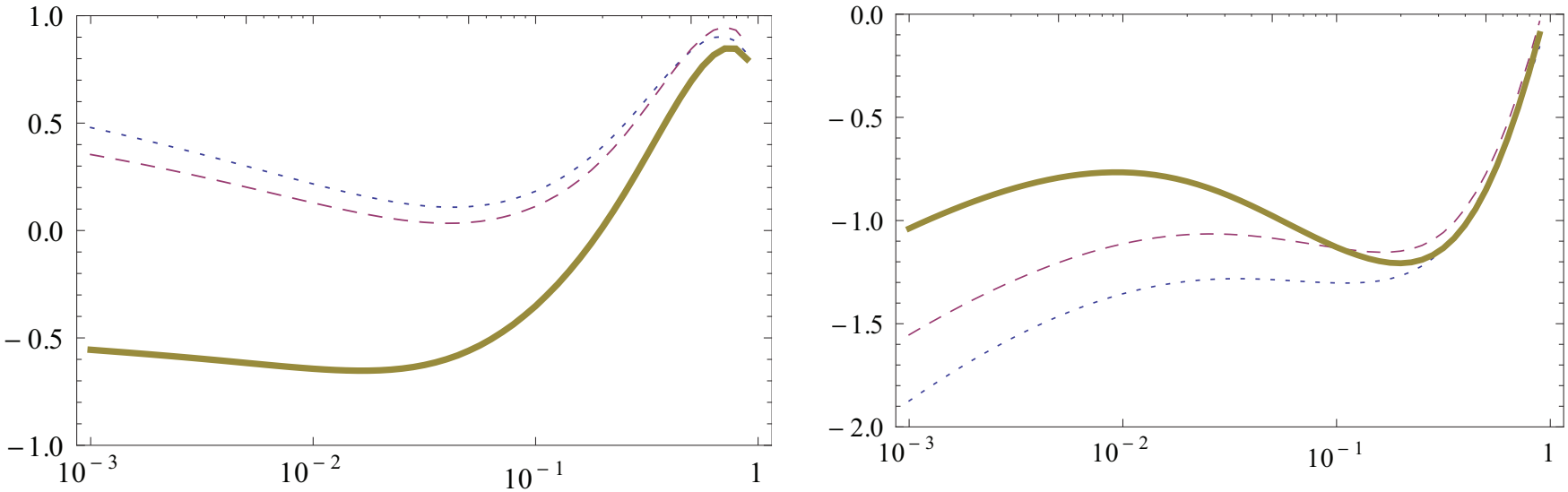

Figure: The real (left) and imaginary(right) parts of the TCS Compton Form Factor $\mathcal{H}$ multiplied by ξ, as a function of ξ in the double distribution model based on MSTW08 parametrization, for $\mu_F^2 = Q^2 = 4$ GeV^2 and $t = -0.1$ GeV^2.

LO : dotted line

LO + NLO-quark : dashed line

LO + NLO-quark + NLO-gluon: solid line

TCS: GK vs MSTW

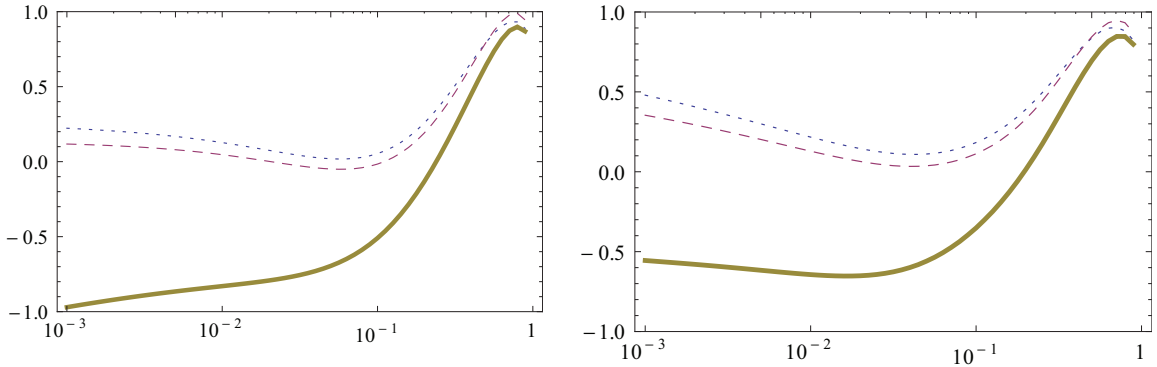

Figure: The real parts of the TCS Compton Form Factor $\mathcal{H}$ multiplied by ξ, as a function of ξ in the double distribution model, for $\mu_F^2 = Q^2 = 4$ GeV^2 and $t = -0.1$ GeV^2. GK- left figure, MSTW- right figure

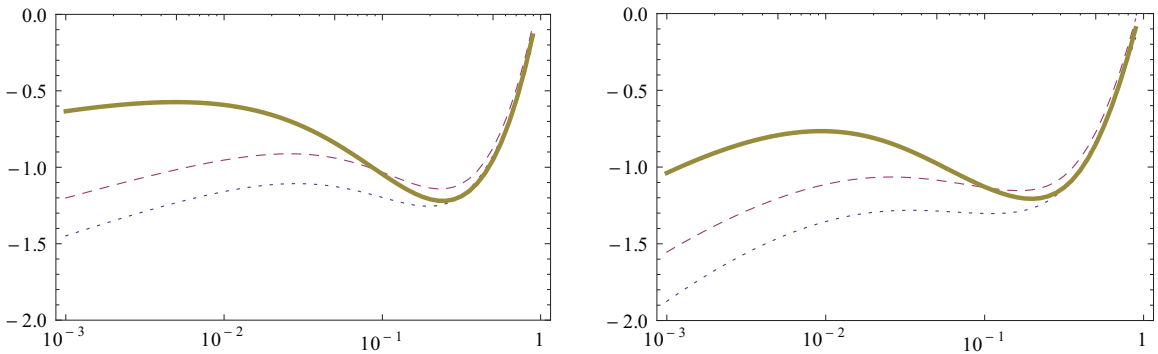

Figure: The imaginary parts of the TCS Compton Form Factor $\mathcal{H}$ multiplied by ξ, as a function of ξ in the double distribution model, for $\mu_F^2 = Q^2 = 4$ GeV^2 and $t = -0.1$ GeV^2. GK- left figure, MSTW- right figure

LO: dotted line LO + NLO-quark: dashed line LO + NLO-quark +NLO-gluon: solid line

DVCS: Re vs. Im parts of DVCS FF

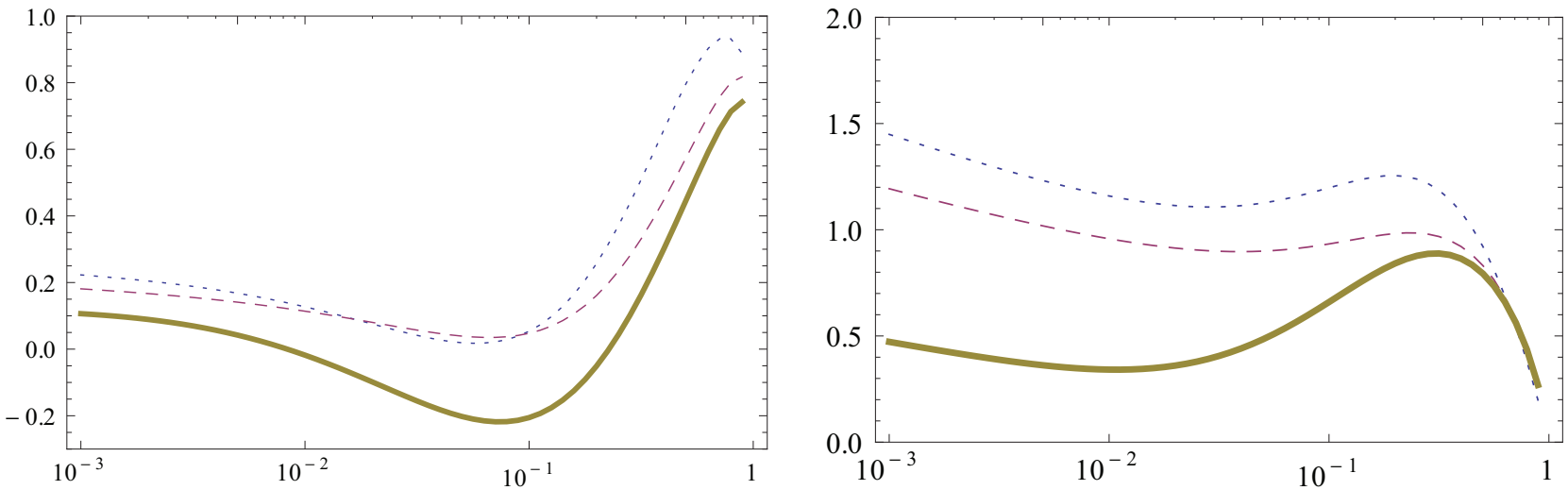

Figure: The real (left) and imaginary(right) parts of the spacelike Compton Form Factor $\mathcal{H}$ multiplied by ξ, as a function of ξ in the double distribution model based on Goloskokov-Kroll parametrization, for $\mu_F^2 = Q^2 = 4$ GeV^2 and $t = -0.1$ GeV^2.

LO: dotted line LO + NLO-quark: dashed line LO + NLO-quark +NLO-gluon: solid line

DVCS: Observables for JLab

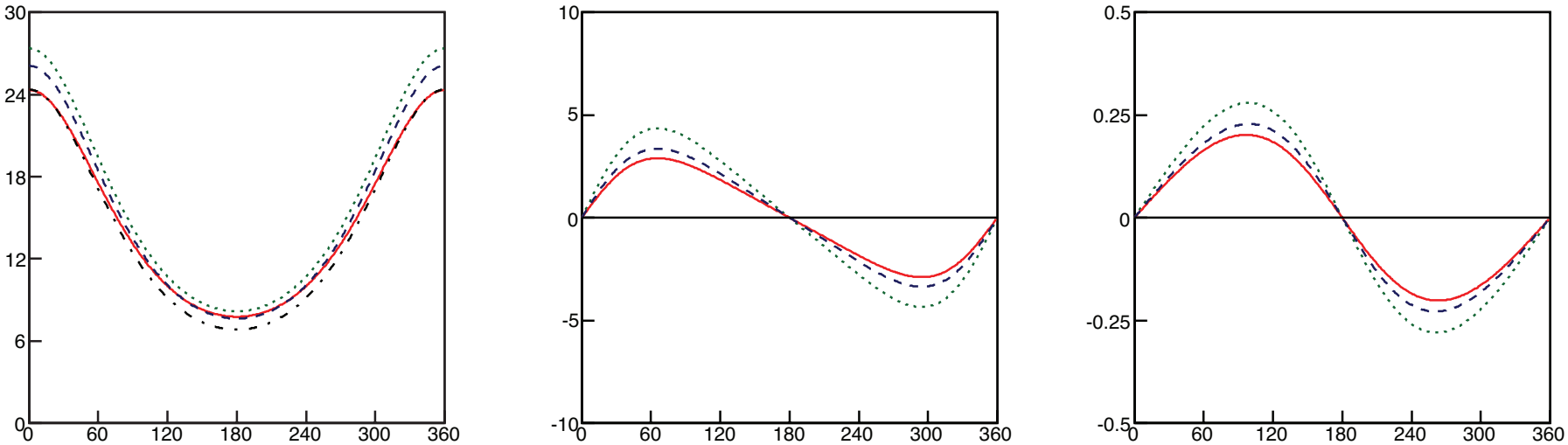

Figure: From left to right, the total DVCS cross section in pb/GeV^4, the difference of cross sections for opposite lepton helicities in pb/GeV^4, the corresponding asymmetry, all as a function of the usual ϕ angle (in Trento conventions) for $E_e = 11$ GeV; $\mu_F^2 = Q^2 = 4$ GeV^2 and t = - 0.2 GeV^2. The GPD $H(x;\xi;t)$ is parametrized by the GK model. The contributions from other GPDs are not included. The Bethe-Heitler contribution appears as the dash-dotted line in the cross section plots (left part)

LO: dotted line LO + NLO-quark: dashed line LO + NLO-quark +NLO-gluon: solid line

DVCS: Observables for COMPASS

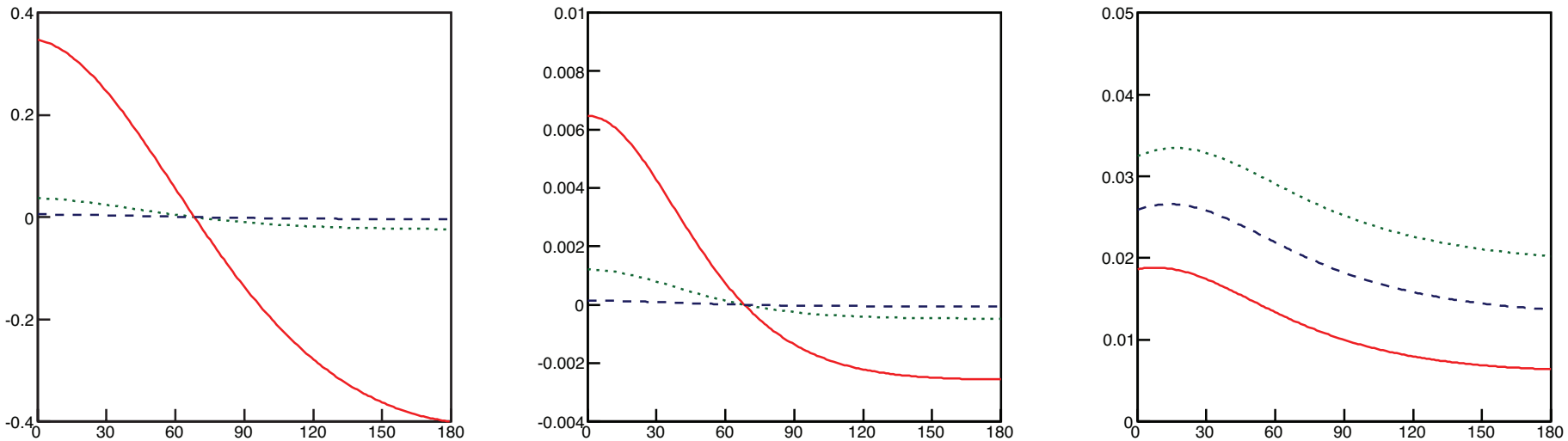

Figure: From left to right: mixed charge-spin asymmetry, mixed charge-spin difference and mixed charge-spin sum in nb/GeV^4. The kinematical point is chosen as $\xi = 0.05$, $Q^2 = 4$ GeV^2, $-t = 0.2$ GeV^2. The GPD $H(x;\xi;t)$ is parametrized by the GK model. The contributions from other GPDs are not included.

$$\mathcal{A}_{CS,U}(\phi) \equiv \frac{\mathcal{D}_{CS,U}}{\mathcal{S}_{CS,U}}\,, \qquad \mathcal{D}_{CS,U}(\phi) \equiv d\sigma^{\overset{+}{\rightarrow}} - d\sigma^{\overset{-}{\leftarrow}}\,, \qquad \mathcal{S}_{CS,U}(\phi) \equiv d\sigma^{\overset{+}{\rightarrow}} + d\sigma^{\overset{-}{\leftarrow}}$$

LO: dotted line LO + NLO-quark: dashed line LO + NLO-quark +NLO-gluon: solid line

Ultraperipheral collisions

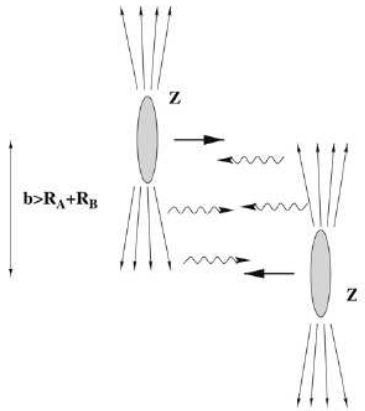

$$\sigma_{pp} = 2 \int \frac{dn(k)}{dk} \sigma_{\gamma p}(k) dk$$

$\sigma_{\gamma p}(k)$ is the cross section for the $\gamma p \to p l^+ l^-$ process and k is the γ's energy, and $\frac{dn(k)}{dk}$ is an equivalent photon flux.

For $\theta = [\pi/4, 3\pi/4]$, $\phi = [0, 2\pi]$, $t = [-0.05\,\mathrm{GeV}^2, -0.25\,\mathrm{GeV}^2]$, $Q'^2 = [4.5\,\mathrm{GeV}^2, 5.5\,\mathrm{GeV}^2]$, and photon energies $k = [20, 900]\,\mathrm{GeV}$ we get:

$$\sigma_{pp}^{BH} = 2.9\mathrm{pb}\ .$$

The Compton contribution gives:

$$\sigma_{pp}^{TCS} = 1.9\mathrm{pb}\ .$$

The interference cross section

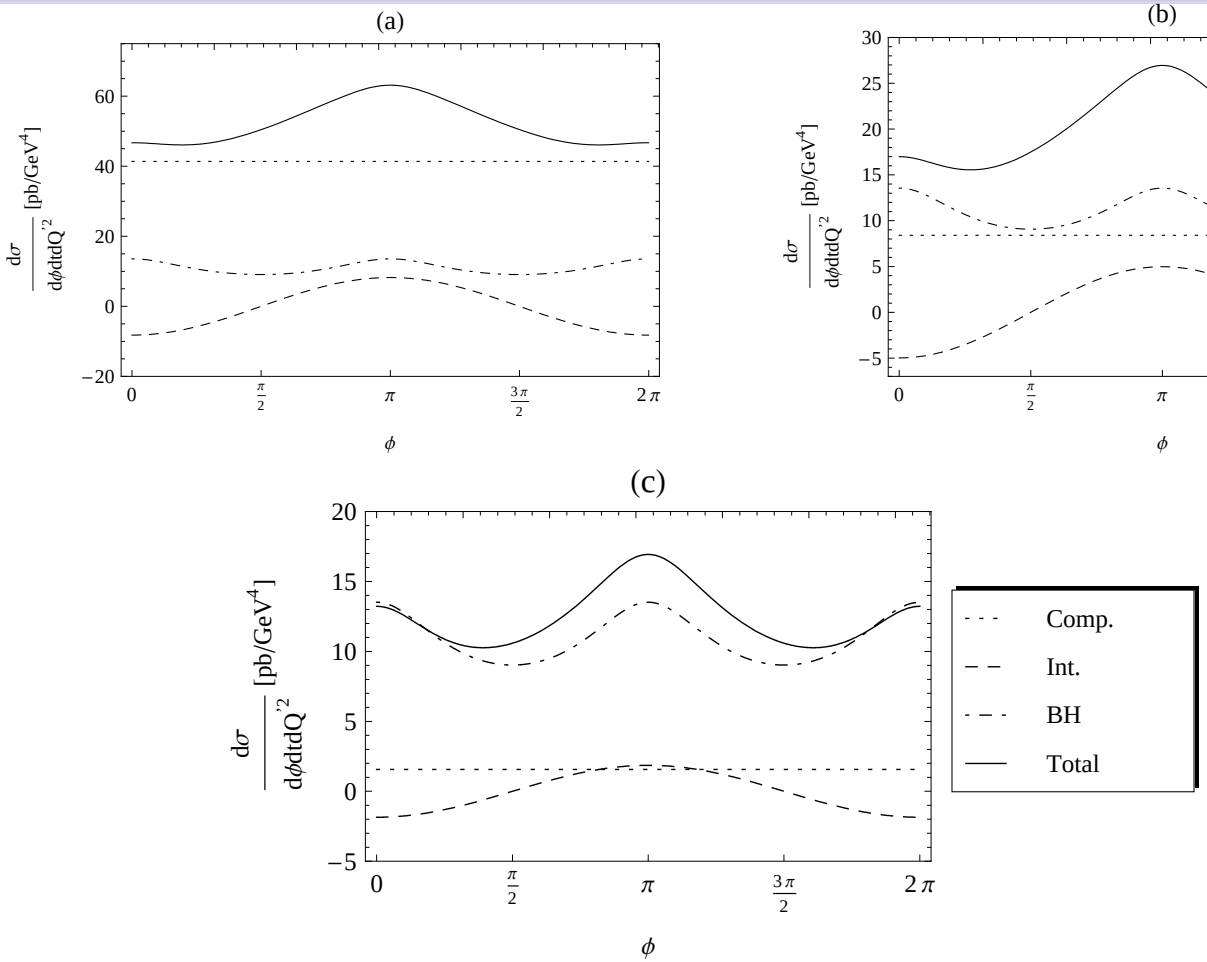

Figure: The differential cross sections (solid lines) for $t = -0.2\,\mathrm{GeV}^2$, $Q'^2 = 5\,\mathrm{GeV}^2$ and integrated over $\theta = [\pi/4, 3\pi/4]$, as a function of φ, for $s = 10^7\,\mathrm{GeV}^2$ (a), $s = 10^5\,\mathrm{GeV}^2$(b), $s = 10^3\,\mathrm{GeV}^2$ (c) with $\mu_F^2 = 5\,\mathrm{GeV}^2$. We also display the Compton (dotted), Bethe-Heitler (dash-dotted) and Interference (dashed) contributions.

Ultraperipheral collisions at RHIC

$L \cdot k \quad \frac{dn}{dk}(\mathrm{mb}^{-1}\mathrm{sec}^{-1})$

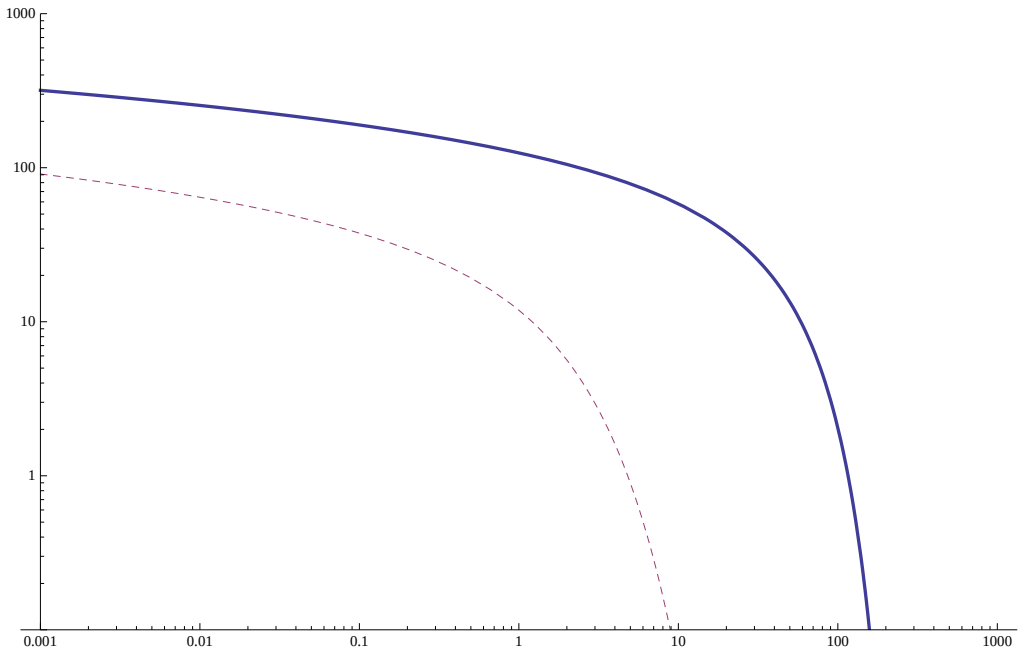

Figure: Effective luminosity of the photon flux from the Au-Au (dashed) and proton-proton (solid) collisions as a function of photon energy k(GeV).

RHIC

$\frac{d\sigma^{AuAu}}{dQ^2 dt d\phi}(\mu\text{b GeV}^{-4})$

J. Wagner

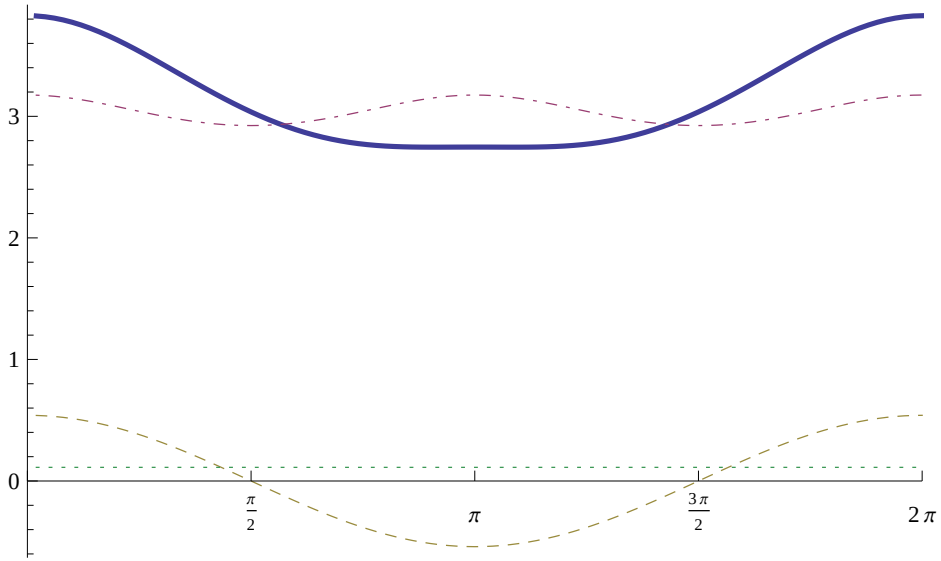

Figure: The differential cross sections (solid lines) for $t = -0.1\,\text{GeV}^2$, $Q'^2 = 5\,\text{GeV}^2$ and integrated over $\theta = [\pi/4, 3\pi/4]$, as a function of φ. We also display the Compton (dotted), Bethe-Heitler (dash-dotted) and Interference (dashed) contributions.

Total BH cross section (for $Q \in (2, 2.9)\,\text{GeV}$, $t \in (-0.2, -0.05)\,\text{GeV}^2$, $\theta = [\pi/4, 3\pi/4]$ and $\phi \in (0, 2\pi)$)

$$\sigma_{BH} = 41\mu\text{b} \qquad \text{Rate} = 0.04\text{Hz}$$

RHIC

$\frac{d\sigma^{pp}}{dQ^2 dt d\phi}(\text{pb GeV}^{-4})$

J. Wagner

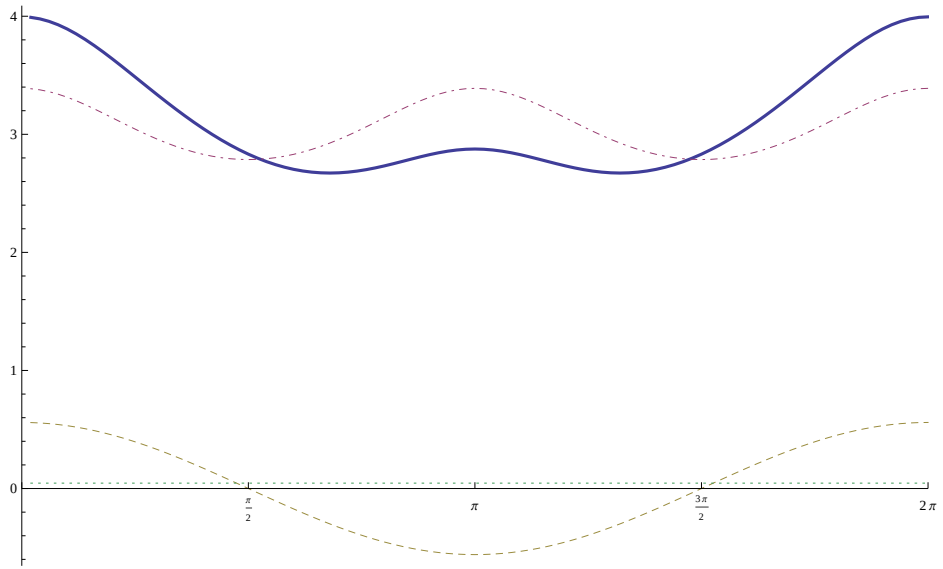

Figure: The differential cross sections (solid lines) for $t = -0.1\,\text{GeV}^2$, $Q'^2 = 5\,\text{GeV}^2$ and integrated over $\theta = [\pi/4, 3\pi/4]$, as a function of φ. We also display the Compton (dotted), Bethe-Heitler (dash-dotted) and Interference (dashed) contributions.

Total BH cross section (for $Q \in (2, 2.9)\,\text{GeV}$, $t \in (-0.2, -0.05)\,\text{GeV}^2$, $\theta = [\pi/4, 3\pi/4]$ and $\phi \in (0, 2\pi)$)

$$\sigma_{BH} = 9\text{pb} \qquad \text{Rate} = 5/\text{day}$$

AFTER@LHC

Ultraperipheral scattering with A Fixed-Target ExpeRiment at the LHC

AFTER@LHC

Ultraperipheral scattering with A Fixed-Target ExpeRiment at the LHC

Motivation for AFTER@LHC:

"A Fixed-Target ExpeRiment at the LHC (AFTER@LHC) : luminosities, target polarisation and a selection of physics studies," PoS QNP **2012** (2012) 049 [arXiv:1207.3507 [hep-ex]]

"Ultra-relativistic heavy-ion physics with AFTER@LHC," arXiv:1211.1294 [nucl-ex]

AFTER@LHC

Ultraperipheral scattering with A Fixed-Target ExpeRiment at the LHC

Motivation for AFTER@LHC:

"A Fixed-Target ExpeRiment at the LHC (AFTER@LHC) : luminosities, target polarisation and a selection of physics studies," PoS QNP **2012** (2012) 049 [arXiv:1207.3507 [hep-ex]]

"Ultra-relativistic heavy-ion physics with AFTER@LHC," arXiv:1211.1294 [nucl-ex]

A. Rakotozafindrabe[a] , R. Arnaldi[b], S.J. Brodsky[c] , V. Chambert[d], J.P. Didelez[d], B. Genolini[d], E.G. Ferreiro[e], F. Fleuret[f], C. Hadjidakis[d], J.P. Lansberg[d], P. Rosier[d], I. Schienbein[g], E. Scomparin[b], U.I. Uggerhï¿½j[h]

[a] IRFU/SPhN, CEA Saclay, 91191 Gif-sur-Yvette Cedex, France
[b] INFN Sez. Torino, Via P. Giuria 1, I-10125, Torino, Italy
[c] SLAC National Accelerator Laboratory, Theoretical Physics, Stanford U., Menlo Park, CA 94025, USA
[d] IPNO, Universitï¿½e Paris-Sud, CNRS/IN2P3, F-91406, Orsay, France
[e] Departamento de Fï¿½ï¿½sica de Partï¿½ï¿½culas, Universidade de Santiago de C., 15782 Santiago de C., Spain
[f] Laboratoire Leprince Ringuet, ï¿½Ecole Polytechnique, CNRS/IN2P3, 91128 Palaiseau, France
[g] LPSC, Universitï¿½e Joseph Fourier, CNRS/IN2P3/INPG, F-38026 Grenoble, France
[h] Department of Physics and Astronomy, University of Aarhus, Denmark

AFTER@LHC Kinematics

Case 1 : proton beam on lead (Pb) target, $\sqrt{s} = 115\,\mathrm{GeV}$, $\epsilon = 1$

Case 2 : lead (Pb) beam on proton target, $\sqrt{s} = 72\,\mathrm{GeV}$, $\epsilon = -1$

$$p = \frac{\sqrt{s}}{2}(1, 0, 0, \epsilon\alpha) \qquad p_A = \frac{\sqrt{s}}{2}(1, 0, 0, -\epsilon\alpha)$$

$$q = x_\gamma \frac{\sqrt{s}}{2}(1, 0, 0, -\epsilon)$$

$$q' = (q'_0, q'_\perp, q'_z) \qquad p' = (p'_0, p'_\perp, p'_z)$$

where $\alpha = \sqrt{1 - \frac{4*M^2}{s}}$

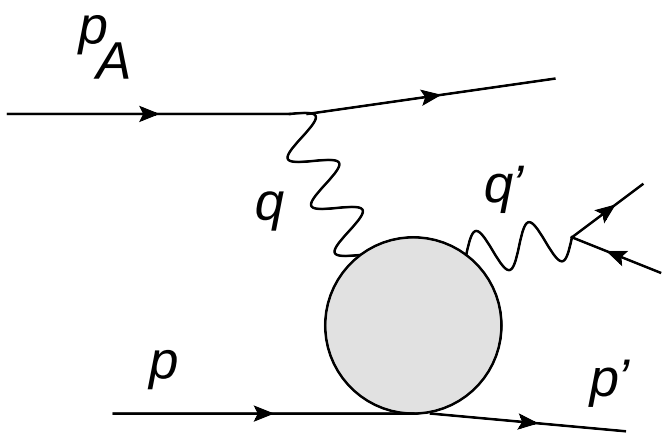

AFTER@LHC Kinematics

Flux of γ's: Baltz et al, Phys. Rep. 458

$$\frac{dn}{dx_\gamma} = \frac{2Z^2\alpha_{EM}}{\pi x_\gamma}\left[\omega^{pA}K_0(\omega^{pA})K_1(\omega^{pA}) - \frac{{\omega^{pA}}^2}{2}\left(K_1^2(\omega^{pA}) - K_0^2(\omega^{pA})\right)\right]$$

where: $\omega^{pA} = x_\gamma M_p(r_p + R_A)$.

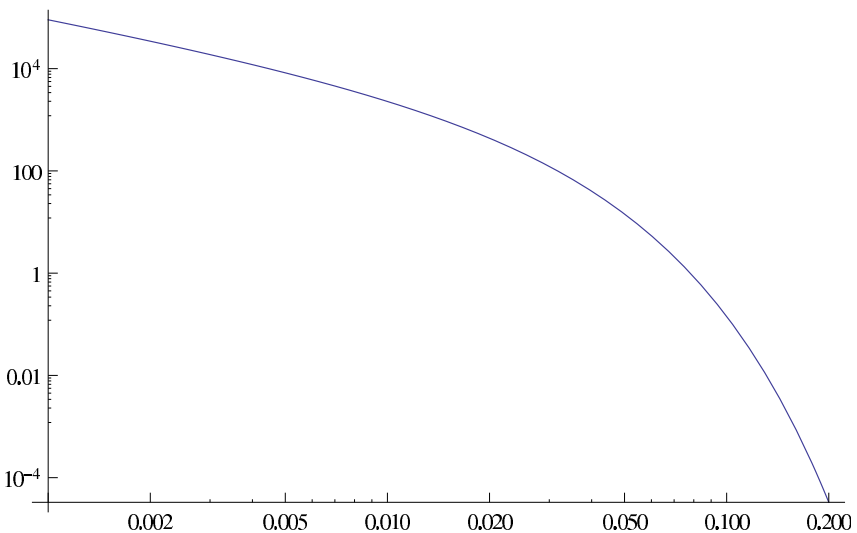

Figure: $\frac{dn}{dx_\gamma}$

AFTER@LHC Kinematics

Rapidity of the outgoing photon::

$$y = \frac{1}{2}\log\frac{q_0' + q_z'}{q_0' - q_z'} = \epsilon\frac{1}{2}\log\left[\frac{(Q^2 - t)(\alpha + 1)}{Q^2(\alpha - 1) - t(\alpha - 1 - 2x) + sx_\gamma^2(\alpha + 1)}\right]$$

Inverting we get:

$$\frac{dx_\gamma}{dy} = \frac{(-2\epsilon)(Q^2 - t)(\alpha + 1)e^{-2\epsilon y}}{\sqrt{4t^2 - 4s(Q^2 - t)(\alpha + 1)\left((\alpha - 1) - (\alpha + 1)e^{-2\epsilon y}\right)}}$$

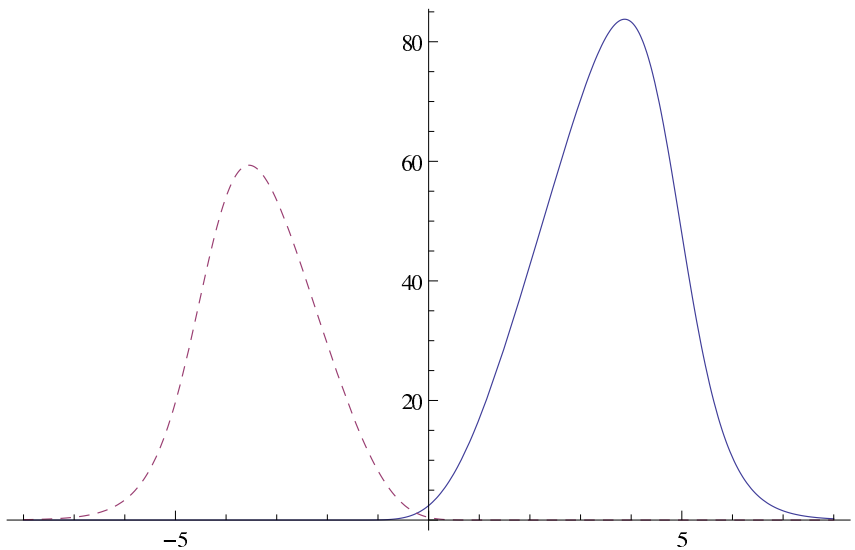

Figure: $\left|\frac{dn}{dy}\right|$,Case 1(solid) and case 2(dashed).

AFTER@LHC Cross-sections

We consider Bethe-Heitler, TCS, and Interference term.

They are functions of $s_{p\gamma}$, t, Q, ϕ, θ.

We integrate over $\theta \in (\pi/4, 3\pi/4)$, in the region where the TCS/BH is the best seen.

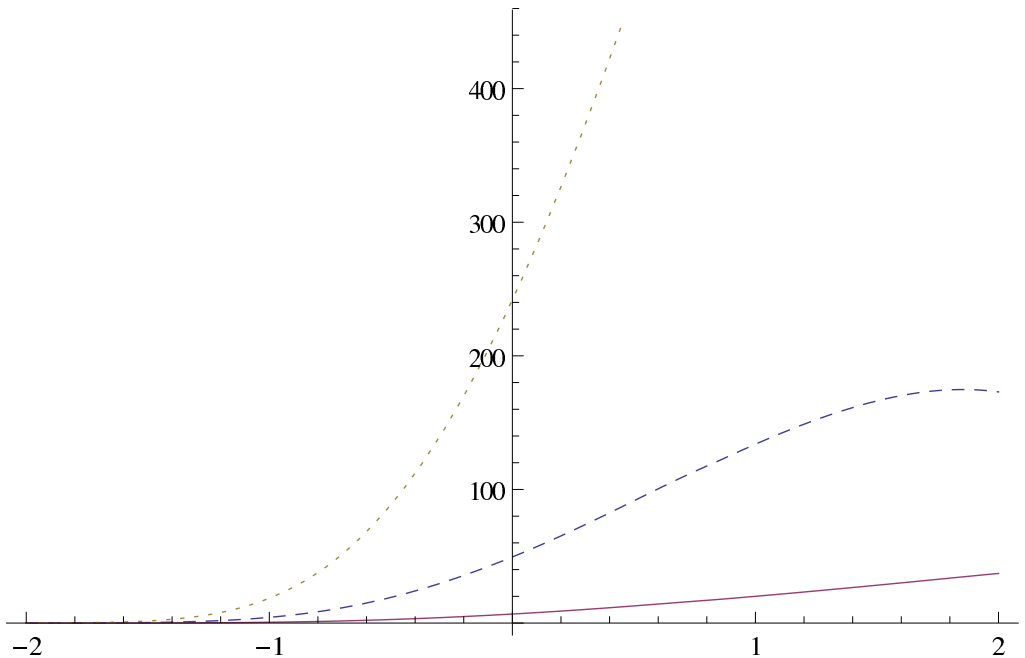

Figure: Case 1 (p beam on Pb target): $\frac{d\sigma}{dQ^2 dt dy d\phi}$ in $pb/\,\mathrm{GeV}^4$ for BH(dotted), TCS(solid), Interference(dashed) as a function of y (in CMS) for $Q^2 = 4\,\mathrm{GeV}^2$, $t = -0.1\,\mathrm{GeV}^2$, $\phi = 0$.

AFTER@LHC Cross-sections

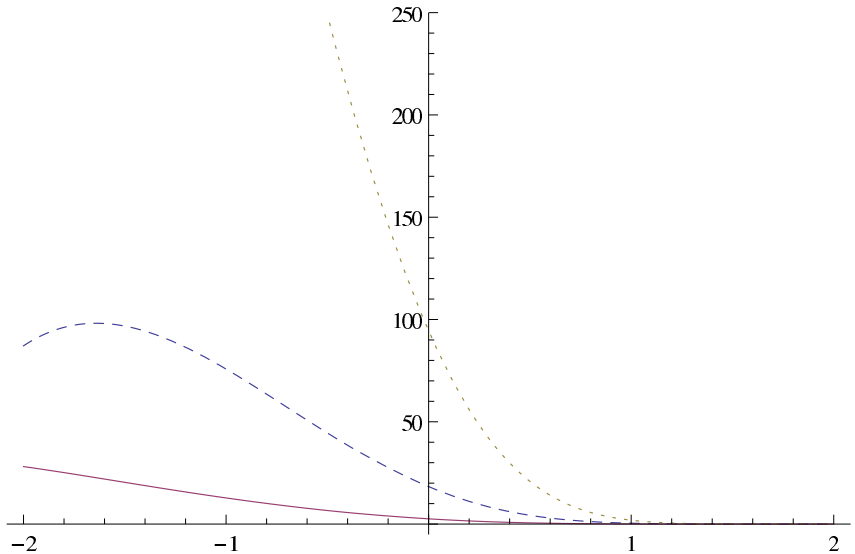

Figure: Case 2 (Pb beam on p target): $\frac{d\sigma}{dQ^2 dt dy d\phi}$ in $pb/\,\mathrm{GeV}^4$ for BH(dotted), TCS(solid), Interference(dashed) as a function of y (in CMS) for $Q^2 = 4\,\mathrm{GeV}^2$, $t = -0.1\,\mathrm{GeV}^2$, $\phi = 0$.

Summary

- TCS already measured in JLAB 6 GeV, but much richer and more interesting kinematical region available after upgrade to 12 GeV.
- Big NLO corrections from gluon sector,
- Better understanding of large terms is needed - factorization scheme? resummation ?
- Compton scattering in ultraperipheral collisions at hadron colliders opens a new way to measure generalized parton distributions
- TCS is an experimentally challenging study at JLab, COMPASS, RHIC and LHC, in many cases due to limitations of original detectors

Summary

- TCS already measured in JLAB 6 GeV, but much richer and more interesting kinematical region available after upgrade to 12 GeV.
- Big NLO corrections from gluon sector,
- Better understanding of large terms is needed - factorization scheme? resummation ?
- Compton scattering in ultraperipheral collisions at hadron colliders opens a new way to measure generalized parton distributions
- TCS is an experimentally challenging study at JLab, COMPASS, RHIC and LHC, in many cases due to limitations of original detectors
- so we look forward for these studies at **AFTER@LHC**

MERCI BEAUCOUP POUR VOTRE ATTENTION